Sialylation on O-glycans protects platelets from clearance by liver Kupffer cells

Yun Li[a,b,1], Jianxin Fu[a,c,1], Yun Ling[a,d,1], Tadayuki Yago[c], J. Michael McDaniel[c], Jianhua Song[c], Xia Bai[a,b], Yuji Kondo[c], Yannan Qin[c,e], Christopher Hoover[c], Samuel McGee[c], Bojing Shao[c], Zhenghui Liu[c], Roberto Sonon[f], Parastoo Azadi[f], Jamey D. Marth[g], Rodger P. McEver[c,h], Changgeng Ruan[a,b], and Lijun Xia[a,b,c,h,2]

[a]Jiangsu Institute of Hematology, Key Laboratory of Thrombosis and Hemostasis of Ministry of Health, The First Affiliated Hospital of Soochow University, Suzhou, Jiangsu 215006, China; [b]Collaborative Innovation Center of Hematology, Soochow University, Suzhou 215006, China; [c]Cardiovascular Biology Research Program, Oklahoma Medical Research Foundation, Oklahoma City, OK 73104; [d]The First People's Hospital of Changzhou, Changzhou, Jiangsu 213000, China; [e]Department of Cell Biology and Genetics, School of Basic Medical Science, Xi'an Jiaotong University Health Science Center, Xi'an 710061, China; [f]Complex Carbohydrate Research Center, University of Georgia, Athens, GA 30602; [g]Department of Molecular, Cellular, and Developmental Biology, University of California, Santa Barbara, CA 93106; and [h]Department of Biochemistry and Molecular Biology, University of Oklahoma Health Sciences Center, Oklahoma City, OK 73104

Edited by Barry S. Coller, The Rockefeller University, New York, NY, and approved June 23, 2017 (received for review May 10, 2017)

Most platelet membrane proteins are modified by mucin-type core 1-derived glycans (O-glycans). However, the biological importance of O-glycans in platelet clearance is unclear. Here, we generated mice with a hematopoietic cell-specific loss of O-glycans (HC *C1galt1*$^{-/-}$). These mice lack O-glycans on platelets and exhibit reduced peripheral platelet numbers. Platelets from HC *C1galt1*$^{-/-}$ mice show reduced levels of α-2,3-linked sialic acids and increased accumulation in the liver relative to wild-type platelets. The preferential accumulation of HC *C1galt1*$^{-/-}$ platelets in the liver was reduced in mice lacking the hepatic asialoglycoprotein receptor [Ashwell–Morell receptor (AMR)]. However, we found that Kupffer cells are the primary cells phagocytosing HC *C1galt1*$^{-/-}$ platelets in the liver. Our results demonstrate that hepatic AMR promotes preferential adherence to and phagocytosis of desialylated and/or HC *C1galt1*$^{-/-}$ platelets by the Kupffer cell through its C-type lectin receptor CLEC4F. These findings provide insights into an essential role for core 1 O-glycosylation of platelets in their clearance in the liver.

platelet | O-glycan | clearance | Kupffer cell

Platelets are essential for normal hemostasis (1) and also play important roles in vascular development/function (2, 3), inflammation, and immune responses (4). Platelets are primarily produced by megakaryocytes in the bone marrow and are the second most abundant circulating blood cells. After entering the circulation, platelets usually live only 3–5 d in mice and 7–10 d in humans before they are cleared (5). Multiple mechanisms control platelet clearance, including antibody and/or T-cell–dependent immune mechanisms (6–8), and platelet apoptosis (9, 10). Recently, glycan modifications have been found to regulate platelet clearance (7, 11–16). Most platelet membrane proteins are glycoproteins, such as GPIbα, GPIIb/IIIa, and GPVI. Platelet glycoproteins are commonly modified by complex carbohydrates including N-linked glycans (N-glycans) and mucin-type O-linked glycans (O-glycans) (17–20). Both N- and O-glycans are commonly "capped" by sialic acids. Desialylation of N-glycans on platelets is important for their removal in the liver. Desialylated platelets are reportedly cleared by hepatocytes via the hepatic asialoglycoprotein receptor (ASGPR) (also called the Ashwell–Morell receptor (AMR); hereafter AMR) (7, 12, 13, 15, 16), a transmembrane protein with two subunits that bind to terminal Gal or GalNAc of desialylated glycans (21). This mechanism contributes to thrombocytopenia associated with sepsis, and anti-GPIbα–mediated immune thrombocytopenia (7, 13).

Although most platelet glycoproteins contain high levels of O-glycans (22, 23), the biological importance of O-glycosylation in platelet clearance is unclear. O-glycosylation starts with the addition of GalNAc to either serine or threonine to form the basic Tn antigen structure (GalNAcα-*O*-Ser/Thr), which is the precursor for the extended and branched complex sialylated O-glycans (24). The most common are the core 1-derived O-glycans (hereafter O-glycans) that include the primary core 1 structure (Galβ3GalNAcα-*O*-Ser/Thr) and its derivatives such as sialylated core 1, extended core 1, and core 2 structures, which are the predominant forms of O-glycans in hematopoietic cells including megakaryocytes/platelets (25).

Core 1 β1,3-galactosyltransferase (C1GALT1, T-synthase) catalyzes the formation of core 1 O-glycans (25–29). We generated mice lacking *C1galt1* specifically in hematopoietic cells (HC *C1galt1*$^{-/-}$). HC *C1galt1*$^{-/-}$ mice exhibit a reduced life-span and increased clearance of platelets in the liver due to defective sialylation. We found that Kupffer cells play a major role in clearing desialylated WT platelets and HC *C1galt1*$^{-/-}$ platelets in cooperation with AMR-expressing hepatocytes. This study provides insights into how sialylated O-glycans regulate platelet homeostasis and clearance.

Results

Mice Lacking Core 1-Derived O-Glycans in Hematopoietic Cells (HC *C1galt1*$^{-/-}$) Exhibit Increased Platelet Clearance in the Liver. To confirm the hematopoietic cell-specific deletion of O-glycans in HC *C1galt1*$^{-/-}$ mice, we first analyzed tissues by immunohistochemical staining with a mAb detecting Tn antigen, which should be exposed in tissues lacking core 1 O-glycans. Anti-Tn stained hematopoietic cells including megakaryocytes, but not vascular

Significance

Although many platelet glycoproteins, such as GPIbα and GPIIb/IIIa, are predominately modified by O-glycans, the biological importance of O-glycans in platelet homeostasis is unclear. Here, we report that platelets lacking O-glycans exhibit a reduced life-span and increased clearance in the liver due to defective sialylation. We found that Kupffer cells play a major role in clearing desialylated O-glycan–deficient platelets in cooperation with hepatocytes via the hepatic asialoglycoprotein receptor. These findings reveal how O-glycosylation regulates platelet homeostasis and clearance; they may also provide insights into the pathogenesis of disorders with thrombocytopenia such as sepsis and immune thrombocytopenia refractory to splenectomy.

Author contributions: Y. Li, J.F., Y. Ling, T.Y., C.R., and L.X. designed research; Y. Li, J.F., Y. Ling, T.Y., J.M.M., J.S., Y.K., C.H., S.M., B.S., Z.L., R.S., and P.A. performed research; X.B. and J.D.M. contributed new reagents/analytic tools; Y. Li, J.F., Y. Ling, T.Y., Y.Q., R.S., P.A., J.D.M., R.P.M., and L.X. analyzed data; and T.Y. and L.X. wrote the paper.

The authors declare no conflict of interest.

This article is a PNAS Direct Submission.

[1]Y. Li, J.F., and Y. Ling contributed equally to this work.

[2]To whom correspondence should be addressed. Email: lijun-xia@omrf.org.

This article contains supporting information online at www.pnas.org/lookup/suppl/doi:10.1073/pnas.1707662114/-/DCSupplemental.

endothelial cells and other cell types, in the HC *C1galt1*$^{-/-}$ tissues (*SI Appendix*, Fig. S1). WT tissues were also negative for Tn staining. In addition, Western blots using bone marrow cell lysates confirmed the efficient and specific deletion of C1galt1 in hematopoietic cells, but not in nonhematopoietic cells such as hepatocytes. Flow-cytometric analysis detected Tn antigens on peripheral blood cells, including red blood cells (RBCs), neutrophils, lymphocytes, and platelets, from HC *C1galt1*$^{-/-}$ but not WT mice. Anti-sialyl Tn Ab did not react with HC *C1galt1*$^{-/-}$ platelets, but reacted with HC *C1galt1*$^{-/-}$ platelets after in vitro sialylation (treated with ST6GalNAcI and CMP-sialic acids), indicating that exposed Tn antigens on HC *C1galt1*$^{-/-}$ platelets are not sialylated.

Further glycan structure analysis (*SI Appendix*, Figs. S2 and S3) indicates that WT platelets contained O-glycans such as sialylated (NeuAc and NeuGc) core 1 and core 2 structures [Galβ1-3(GlcNAcβ1-6)GalNAc] at *m/z* 896, 926, 1,259, and 1,317, respectively, as well as a fucosylated core 4 at *m/z* 1,794. However, these structures were absent in HC *C1galt1*$^{-/-}$ platelets. A residual amount of core 1 O-glycans, which might be from exogenous sources as platelets are known to uptake or bind to glycoproteins in the circulation, was detected in HC *C1galt1*$^{-/-}$ platelets. N-glycan profiles were comparable between WT and HC *C1galt1*$^{-/-}$ platelets, indicating that *C1galt1* loss does not appreciably affect N-glycan biosynthesis. These data indicate that deletion of *C1galt1* specifically abolishes the formation of sialylated core 1-derived O-glycans in platelets.

HC *C1galt1*$^{-/-}$ mice appeared normal, with postnatal growth rate, and life-span similar to that of WT mice. Compared with WT mice, HC *C1galt1*$^{-/-}$ mice showed normal peripheral RBC and leukocyte number but had a reduced number of platelets (Fig. 1*A* and *SI Appendix*, Fig. S4*A*). The percentage of reticulated platelets was significantly higher in blood from HC *C1galt1*$^{-/-}$ mice compared with WT mice, and giant platelets were occasionally observed in Wright-Giemsa–stained blood smears from HC *C1galt1*$^{-/-}$ mice (*SI Appendix*, Fig. S4 *B* and *C*). These results suggest a compensatory enhanced megakaryopoiesis and platelet production in HC *C1galt1*$^{-/-}$ mice. To test whether accelerated platelet clearance plays an important role in the thrombocytopenia in HC *C1galt1*$^{-/-}$ mice, we performed adoptive platelet transfer studies in which 10^8 WT or HC *C1galt1*$^{-/-}$ biotinylated platelets were transfused into WT recipient mice (Fig. 1*B*). HC *C1galt1*$^{-/-}$ platelets were cleared faster than WT platelets, with a major reduction of transfused HC *C1galt1*$^{-/-}$ platelets within the initial 20 min. The half-lives ($t_{1/2}$) of HC *C1galt1*$^{-/-}$ and WT platelets were ∼22 and 50 h, respectively. Furthermore, in vivo biotin labeling experiments show that the clearance of endogenous platelets was also faster in HC *C1galt1*$^{-/-}$ mice than that in WT mice (*SI Appendix*, Fig. S5). These findings indicate that the loss of core 1 O-glycans in platelets results in their increased clearance, leading to reduced peripheral platelet counts in HC *C1galt1*$^{-/-}$ mice.

To determine where HC *C1galt1*$^{-/-}$ platelets are cleared, we immunostained cryosections of different organs, including spleen and liver (Fig. 1*C*). Platelets were detected in the spleen and liver of both HC *C1galt1*$^{-/-}$ and WT mice, supporting that HC *C1galt1*$^{-/-}$ platelets were cleared in both organs. However, the numbers of platelets were comparable in HC *C1galt1*$^{-/-}$ and WT spleen. In contrast, HC *C1galt1*$^{-/-}$ liver displayed nearly threefold more platelets than WT liver. To test whether the liver is a major site for the clearance platelets with O-glycan deficiency in HC *C1galt1*$^{-/-}$ mice, we performed competitive transfusion experiments (Fig. 1*D*). Despite transfusing an equal number of HC *C1galt1*$^{-/-}$ and WT platelets, we detected significantly more CMFDA-labeled HC *C1galt1*$^{-/-}$ platelets than CMRA-labeled WT platelets in WT recipient liver, supporting increased clearance of HC *C1galt1*$^{-/-}$ platelets in the liver compared with WT platelets. These data indicate that HC *C1galt1*$^{-/-}$ platelets are differentially cleared in the liver.

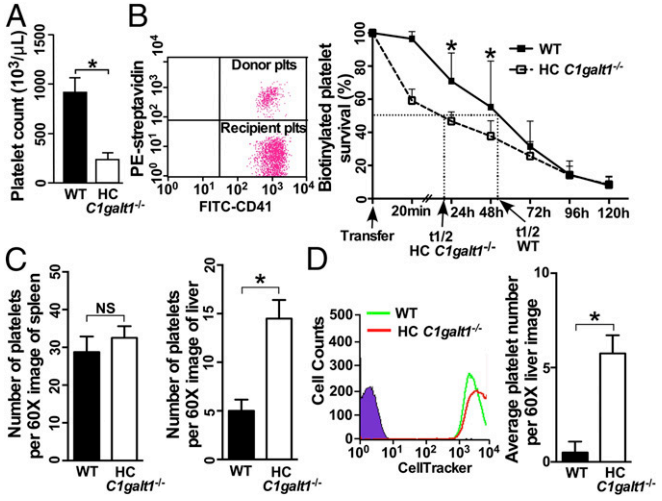

Fig. 1. HC *C1galt1*$^{-/-}$ mice develop thrombocytopenia with reduced platelet life-span, and HC *C1galt1*$^{-/-}$ platelets display a greater clearance than WT platelets in the liver. (*A*) Peripheral platelet count in WT and HC *C1galt1*$^{-/-}$ mice. Data represent means ± SD. $n = 5$ mice. *$P < 0.05$. (*B*) Representative dot plot shows that 10^8 biotinylated platelets from WT mice or HC *C1galt1*$^{-/-}$ mice were adoptively transfused into WT recipients. Peripheral blood samples were taken from recipient mice at 0, 0.3, 24, 48, 72, 96, and 120 h after transfusion. Data represent means ± SD at each time point. $n = 4$ experiments. *$P < 0.05$. (*C*) Bar graphs are quantification of platelets or platelet clusters per 60× image. Data represent mean ± SD. $n = 10$ images/genotype. *$P < 0.05$. (*D*) Flow-cytometric analysis of labeling efficiency of WT and HC *C1galt1*$^{-/-}$ platelets by CellTracker CMRA (red) and CMFDA (green), respectively. Bar graphs are quantification of number of platelets per 60× field in WT recipients 90 min after the competitive transfusion of labeled WT and HC *C1galt1*$^{-/-}$ platelets. $n = 3$ experiments. *$P < 0.05$.

The AMR Contributes to HC *C1galt1*$^{-/-}$ Platelet Clearance. The AMR (ASGPR) mediates the clearance of desialylated platelets by hepatocytes in the liver (7, 12, 13, 15, 16). To investigate the role of AMR in HC *C1galt1*$^{-/-}$ platelet clearance, we performed competitive transfusion assays by simultaneously transfusing CMRA-labeled WT and CMFDA-labeled HC *C1galt1*$^{-/-}$ platelets into either WT or *Asgr1*$^{-/-}$ recipient mice (Fig. 2*A*). WT platelets showed similar survival rates in WT and *Asgr1*$^{-/-}$ recipients. In contrast, the survival rates of transfused HC *C1galt1*$^{-/-}$ platelets increased significantly in *Asgr1*$^{-/-}$ compared with WT recipient mice, at all time points analyzed. Consistent with these results, significantly fewer HC *C1galt1*$^{-/-}$ platelets were detected in *Asgr1*$^{-/-}$ recipient liver compared with WT recipient liver, although more HC *C1galt1*$^{-/-}$ than WT platelets were detected in both recipient livers (Fig. 2*B*). These results support that AMR contributes to the increased clearance of HC *C1galt1*$^{-/-}$ platelets in the liver. To further determine whether AMR contributes to HC *C1galt1*$^{-/-}$ platelet clearance, we generated HC *C1galt1*$^{-/-}$;*Asgr1*$^{-/-}$ double-knockout mice (DKO). These mice displayed a significant increase in peripheral platelet counts relative to HC *C1galt1*$^{-/-}$ mice (Fig. 2*C*), indicating that AMR plays an important role in the increased clearance of HC *C1galt1*$^{-/-}$ platelets in the liver. However, loss of AMR did not completely rescue the reduction of peripheral platelets, suggesting that AMR-independent mechanisms also contribute to HC *C1galt1*$^{-/-}$ platelet clearance in the liver. To determine whether hepatocytes phagocytose HC *C1galt1*$^{-/-}$ platelets mediated by AMR, we performed binding and ingestion assays using the hepatocyte HepG2 cell line, which expresses AMR. CMFDA-labeled platelets were incubated with HepG2 cells,

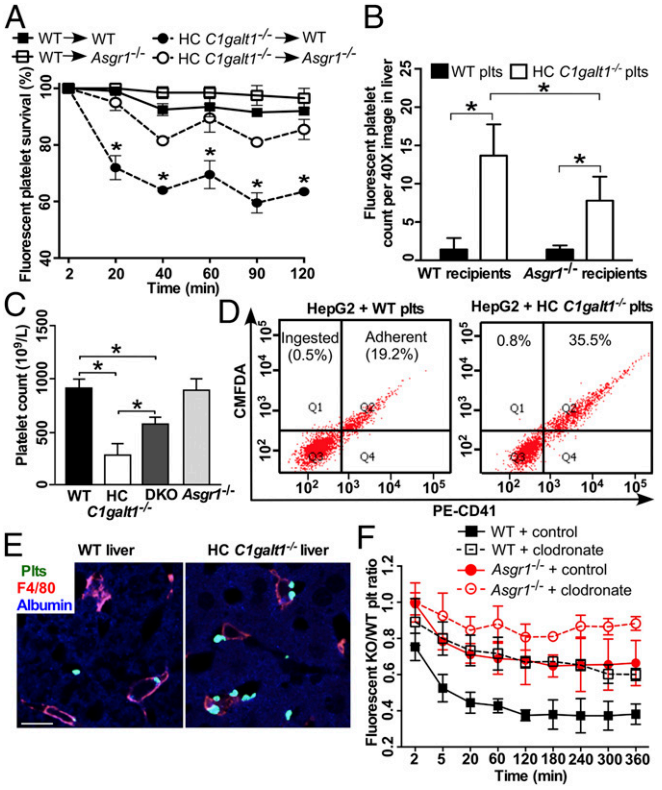

Fig. 2. The AMR participates in HC *C1galt1*$^{-/-}$ platelet clearance. (*A*) Survival percentage of competitively transfused CMRA-labeled WT platelets or CMFDA-labeled HC *C1galt1*$^{-/-}$ platelets in peripheral blood of either WT or *Asgr1*$^{-/-}$ recipients. $n = 3$ experiments. *$P < 0.05$. (*B*) Quantification of labeled WT or HC *C1galt1*$^{-/-}$ platelets in recipient liver sections. Data are mean ± SD. n equals at least five randomly selected 40× microscopic fields. *$P < 0.05$. (*C*) Peripheral platelet count of WT and HC *C1galt1*$^{-/-}$;*Asgr1*$^{-/-}$ mice. $n = 3$ mice/genotype. *$P < 0.05$. (*D*) Flow-cytometric analysis of HepG2 cell ingestion of CMFDA-labeled platelets. Platelet adherent to HepG2 cells were identified as CD41 and CMFDA double positive. CMFDA single-positive HepG2 cells suggest ingestion of platelets. The dot plots are representative of five experiments. (*E*) Representative images of immunostaining of platelets (anti-thrombocyte serum, green), Kupffer cells (F4/80, red), and hepatocytes (albumin, blue) in liver sections. (Scale bar, 10 μm.) (*F*) The ratio of competitively transfused fluorescent HC *C1galt1*$^{-/-}$ platelets to WT platelets in peripheral blood of WT and *Asgr1*$^{-/-}$ recipients with or without Kupffer cell depletion. Data are mean ± SD at each time point. $n =$ 6 mice per group.

washed, and stained with PE–anti-CD41 for flow cytometry analysis (Fig. 2*D*). We found that more CMFDA and CD41 double-positive HC *C1galt1*$^{-/-}$ platelets adhered to HepG2 cells than WT platelets did. However, almost no single CMFDA-positive platelets were detected within HepG2 cells incubated with either HC *C1galt1*$^{-/-}$ or WT platelets (Fig. 2*D*, "ingested"), suggesting that HepG2 did not phagocytose platelets under these conditions.

Kupffer Cells Are the Primary Cells Phagocytosing HC *C1galt1*$^{-/-}$ Platelets. We performed confocal imaging analysis of liver sections from WT and HC *C1galt1*$^{-/-}$ mice to further investigate differential platelet clearance in the liver and found that platelets were primarily associated with Kupffer cells in liver sinusoids of HC *C1galt1*$^{-/-}$ mice (Fig. 2*E*). In contrast, platelets were rarely found to be associated with hepatocytes. Confocal imaging analysis did not detect any other blood cells such as RBCs associated with Kupffer cells in the HC *C1galt1*$^{-/-}$ liver (*SI Appendix*, Fig. S6).

To determine whether Kupffer cells are critical for HC *C1galt1*$^{-/-}$ platelet clearance, we performed platelet competitive transfusions in WT or *Asgr1*$^{-/-}$ recipient mice after depletion of macrophages including Kupffer cells with clodronate liposomes. We confirmed depletion of Kupffer cells 2 d after clodronate liposome treatment by immunostaining of liver sections (*SI Appendix*, Fig. S7). Two days after treatment with clodronate or control liposomes, we transfused an equal ratio of CMRA-labeled WT and CMFDA-labeled *HC C1galt1*$^{-/-}$ platelets into recipient mice and monitored platelet clearance. WT mice injected with control liposomes displayed a much lower ratio of transfused HC *C1galt1*$^{-/-}$:WT platelets than WT mice injected with clodronate liposomes (Fig. 2*F*). Thus, macrophage depletion preferentially stabilizes HC *C1galt1*$^{-/-}$ platelets. Furthermore, the ratio of transfused HC *C1galt1*$^{-/-}$:WT platelets was almost normalized to 1 in *Asgr1*$^{-/-}$ mice treated with clodronate liposomes, indicating that macrophage depletion and loss of AMR both stabilize HC *C1galt1*$^{-/-}$ platelets. These data indicate that HC *C1galt1*$^{-/-}$ platelets were primarily cleared by the Kupffer cells and that AMR contributes to the Kupffer cell-mediated clearance.

HC *C1galt1*$^{-/-}$ Platelets Are Deficient in α-2,3-Sialylation. Our data indicate that AMR, which binds to desialylated glycans, is involved in clearing HC *C1galt1*$^{-/-}$ platelets in the liver. Therefore, we analyzed the sialylation profile of HC *C1galt1*$^{-/-}$ platelets. Lectin-binding analyses indicated that the binding of SNA (specific for α-2,6-sialylation), RCA 1 (specific for terminal β-galactose), and Con A (specific for mannose in N-glycans) were similar on HC *C1galt1*$^{-/-}$ platelets relative to WT platelets (Fig. 3*A*). In contrast, MALII (specific for α-2,3-sialylation) binding was decreased for HC *C1galt1*$^{-/-}$ compared with WT platelets. Removal of sialic acids by neuraminidase, but not N-glycans by PNGase F, reduced the binding of MALII to WT platelets (Fig. 3*B*). This result demonstrates that MALII recognizes α-2,3-sialylation, a major form of sialylation, on O-glycans (30). Taken together, our results indicate that a lack of O-glycans considerably reduces α-2,3-sialylation, which corroborates the MALDI-TOF-MS/MS data (*SI Appendix*, Fig. S2).

Many platelet glycoprotein surface receptors such as GPIbα contain high levels of O-glycans (*SI Appendix*, Table S1). We found that O-sialoglycoprotein endopeptidase (OSGE) treatment, which specifically removes GPIbα levels (31), did not change MALII binding (*SI Appendix*, Fig. S8). In addition, OSGE treatment did not significantly change the survival rate of HC *C1galt1*$^{-/-}$ platelets (*SI Appendix*, Fig. S9). These data support that desialylated GalNAc

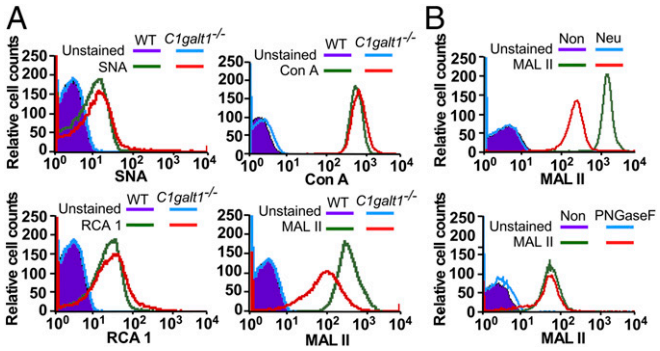

Fig. 3. (*A*) Flow-cytometric analysis of WT and HC *C1galt1*$^{-/-}$ platelets after being stained with lectin SNA (for α-2,6-linked sialic acids), Con A (for mannose in N-glycans), RCA 1 (for galactose exposure), and MALII (for α-2,3-linked sialic acids). Data represent three experiments. (*B*) MALII profile of WT platelets with or without neuraminidase (Neu) or PNGase F treatment. Data represent two experiments.

epitopes on GPIbα are not significantly involved in AMR binding, and exposed GalNAc on GPIbα do not significantly contribute to the AMR-mediated increased clearance of HC *C1galt1*$^{-/-}$ platelets in the liver.

AMR-Expressing Hepatocytes Facilitate the Clearance of Both HC *C1galt1*$^{-/-}$ Platelets and Desialylated Platelets by Kupffer Cells. Previous reports suggested that desialylated platelets are primarily phagocytosed by AMR-expressing hepatocytes (7, 13, 15, 16). We used confocal imaging to compare the localizations of transfused, CMFDA-labeled desialylated WT platelets, which lack α2-3,6,8-sialic acids on both N- and O-glycans after neuraminidase treatment, or CMFDA-labeled HC *C1galt1*$^{-/-}$ platelets in the liver. Both desialylated WT platelets and HC *C1galt1*$^{-/-}$ platelets were detected to be primarily associated with Kupffer cells in the recipient livers of WT but not *Asgr1*$^{-/-}$ mice (Fig. 4*A*). Further high-resolution confocal imaging and 3D rendering of *z*-stack Kupffer cell images revealed that significant numbers of desialylated or HC *C1galt1*$^{-/-}$ platelets were inside the phagocytic Kupffer cells (Fig. 4 *B* and *C*).

To determine whether AMR is specifically expressed on hepatocytes and mediates the clearance of desialylated or HC *C1galt1*$^{-/-}$ platelets, purified Kupffer cells were analyzed for expression of *Asgr1* transcripts by RT-PCR and AMR protein levels by Western blotting. *Asgr1* expression was detected in RNA isolated from WT but not *Asgr1*$^{-/-}$ liver, verifying the specificity of the RT-PCR analysis (Fig. 4*D*). The RT-PCR analysis detected macrophage markers such as *EMR1*, *CD163*, and *CD68* in RNA isolated from purified Kupffer cells, but did not detect expression of *Asgr1*. Consistent with the absence of *Asgr1* mRNA, Western blot analysis did not reveal any AMR protein in Kupffer cells (Fig. 4*E*). These data indicate that Kupffer cells do not express AMR. In addition, platelet does not express AMR (*SI Appendix*, Fig. S10).

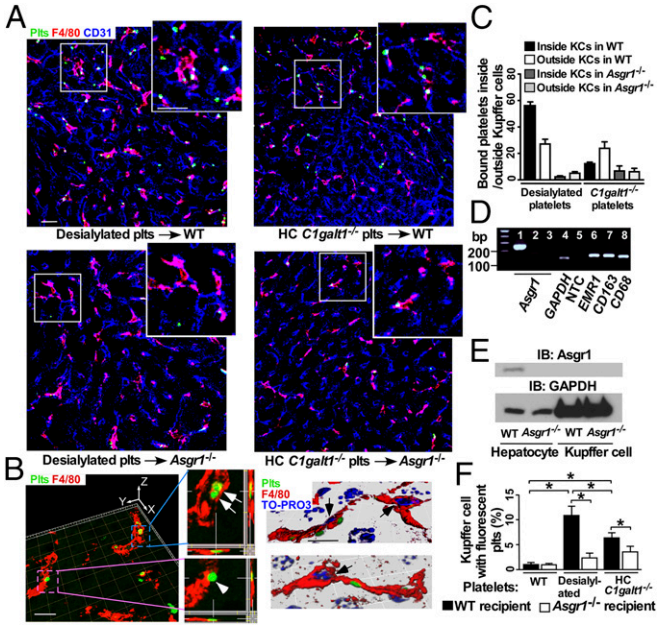

Fig. 4. Desialylated or HC *C1galt1*$^{-/-}$ platelets are associated with Kupffer cells. (*A*) Representative confocal microscopic images showing association of CMFDA-labeled platelets with the Kupffer cell (F4/80 staining) in the liver. Anti-CD31 labels sinusoidal endothelial cells. The upper right inlet in each panel shows the enlarged image indicated by the white square. (Scale bar, 10 μm.) (*B*) A 3D reconstructed image with orthogonal projections of *z* stacks shows platelets phagocytosed (arrows) by or bound to (arrowhead) the Kupffer cell (*Left*), 3D-reconstructed images with nucleus staining by TO-PRO3 (blue). Arrow marks the Kupffer cell nucleus (*Right*). (Scale bar, 5 μm.) (*C*) Quantification of transfused platelets adherent to or inside Kupffer cells in different recipient liver. Data are mean ± SD. $n = 6$–10; 20× confocal microscopic fields. (*D*) RT-PCR analysis of expression of *Asgr1* and of macrophage markers. Lane 1, WT liver; lane 2, *Asgr1*$^{-/-}$ liver; lanes 3–8, sorted WT Kupffer cells. (*E*) Western blot analysis of AMR levels in hepatocytes or Kupffer cells. (*F*) Flow-cytometric analysis of F4/80-positive Kupffer cells from WT and *Asgr1*$^{-/-}$ recipients for association with transfused CMFDA-labeled WT, desialylated, or HC *C1galt1*$^{-/-}$ platelets.

To determine whether hepatocyte AMR contributes to Kupffer cell-mediated phagocytosis of desialylated or HC *C1galt1*$^{-/-}$ platelets, we transfused CMFDA-labeled WT, desialylated WT, or HC *C1galt1*$^{-/-}$ platelets into WT or *Asgr1*$^{-/-}$ recipient mice, and subsequently isolated and analyzed CMFDA-labeled platelet-associated Kupffer cells (Fig. 4*F*). As expected, WT platelets were rarely found to be associated with Kupffer cells in WT recipients or *Asgr1*$^{-/-}$ recipients. However, a higher percentage of desialylated or HC *C1galt1*$^{-/-}$ platelets were associated with Kupffer cells in WT recipients than in *Asgr1*$^{-/-}$ recipients. Together, these data indicate that AMR promotes preferential adherence to and phagocytosis of HC *C1galt1*$^{-/-}$ and desialylated platelets by Kupffer cells.

To obtain further evidence that AMR contributes to platelet clearance by Kupffer cells in the liver, we observed the interactions of transfused, labeled WT, desialylated WT, or HC *C1galt1*$^{-/-}$ platelets with sinusoidal surface and with Kupffer cells at real time using spinning-disk confocal intravital microscopy (Fig. 5 *A*–*C*). Immediately after infusion (early phase), most labeled–desialylated WT or HC *C1galt1*$^{-/-}$ platelets rolled on and/or adhered to the sinusoid surface. Many of these "rolling" platelets subsequently became associated with Kupffer cells (Fig. 5*B*). After 30 min (late phase), significant more desialylated WT or HC *C1galt1*$^{-/-}$ platelets were associated with Kupffer cells. All of these interactions were significantly reduced by i.p. administration of asialofetuin expressing Gal/GalNAc epitopes, which competitively blocks the binding of AMR to desialylated Gal or GalNAc, but not by administration of the control, fetuin, that expresses sialylated Gal and GalNAc epitopes. Further analysis shows that GalNAc epitopes on HC *C1galt1*$^{-/-}$ platelets were not modified by any other potential glycosylation during circulation in recipient mice (*SI Appendix*, Fig. S11).

Kupffer cells express CLEC4F (Fig. 5*D*), which is a member of C-type lectin with high affinity to desialylated glycoproteins with terminal Gal or GalNAc (32). However, it is unknown whether CLEC4F binds to desialylated WT and/or HC *C1galt1*$^{-/-}$ platelets, which express either Gal or GalNAc. To address this question, we knocked down CLEC4F in Kupffer cells isolated from WT mice using siRNA, and measured desialylated WT or HC *C1galt1*$^{-/-}$ platelet binding. CLEC4F-specific siRNA resulted in an over 85% reduction of CLEC4F on Kupffer cells (Fig. 5*D*). Significantly more desialylated WT or HC *C1galt1*$^{-/-}$ platelets bound to WT Kupffer cells compared with mock-treated platelets (Fig. 5*E*). After knockdown of CLEC4F, the binding of desialylated WT or HC *C1galt1*$^{-/-}$ platelets was reduced to 40–50%. Pretreatment of Kupffer cells with Gal or GalNAc polymers, which competes for binding to the CLEC4F, further reduced the desialylated WT or HC *C1galt1*$^{-/-}$ platelet binding to the levels of mock-treated WT platelets, indicating that the Kupffer cell CLEC4F is a major specific receptor for either Gal epitopes on desialylated WT platelets, or GalNAc epitopes on HC *C1galt1*$^{-/-}$ platelets. These results support that hepatocyte AMR coordinates the clearance of desialylated and HC *C1galt1*$^{-/-}$ platelets by Kupffer cells through the CLEC4F receptor.

Discussion

We have uncovered an important role of a major post-translational modification, O-glycosylation, in platelet homeostasis. Many platelet glycoproteins are modified by O-glycans; we show that HC *C1galt1*$^{-/-}$ platelets lacking O-glycans have a

MEDICAL SCIENCES

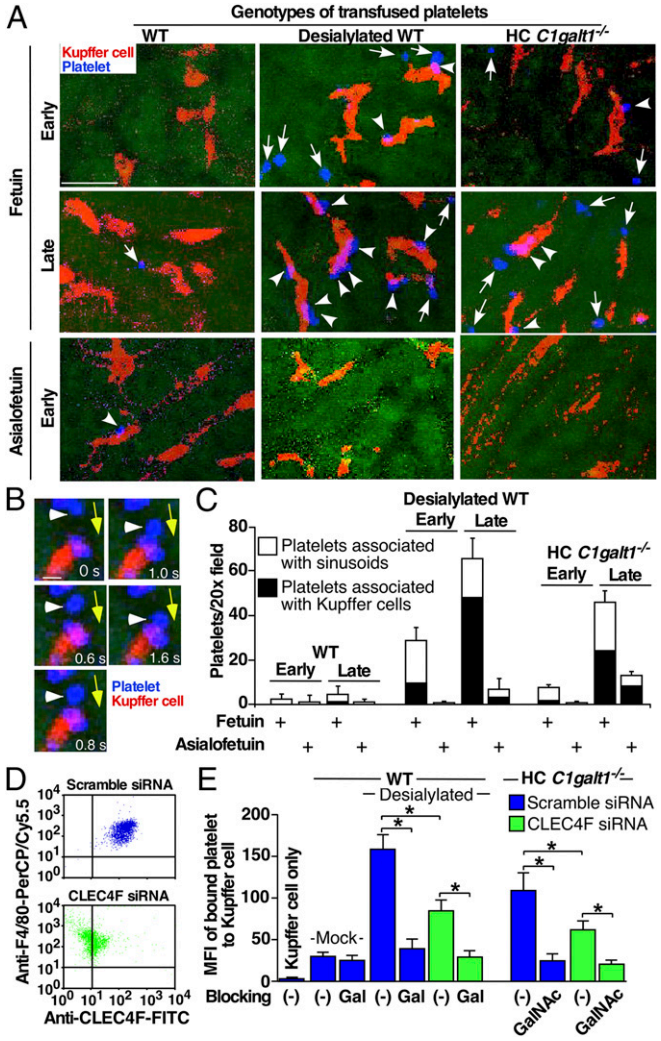

Fig. 5. Confocal intravital microscopy of recipient livers transfused with WT, desialylated, or HC *C1galt1*$^{-/-}$ platelets. (*A*) Representative confocal intravital images of the WT recipient liver at 20-s (early) or 30-min (late) time points after transfusion of platelets labeled with CellTracker (blue). Recipients were administered with fetuin or asialofetuin (i.p.) before platelet transfusions. The Kupffer cells were labeled by an injection of PE-anti-F4/80 (i.v.) before transfusion (red). Arrows indicate transfused platelets associated with sinusoidal endothelium. Arrowheads show Kupffer cells associated with transfused platelets. (Scale bar, 10 μm.) (*B*) Representative serial images at indicated time frames (in seconds) of a platelet (arrowhead) first rolling on the sinusoid surface and then interacting with a Kupffer cell. Yellow arrows mark the direction of blood flow. (Scale bar, 2 μm.) (*C*) Quantification of interactions of platelets with liver sinusoid surface and with Kupffer cells (KCs) at different time points after platelet transfusion. $n = 5$–10 images/time point. Data represent means ± SD from three experiments. (*D*) Expression of CLEC4F on F4/80-positive Kupffer cells from WT mice transfected with scramble or CLEC4F-specific siRNA measured by flow cytometry. (*E*) Flow-cytometric analysis of binding of PHK26-labeled mock-treated or sialidase-treated (desialylated) platelets or HC *C1galt1*$^{-/-}$ platelets to Kupffer cells transfected with either scramble or CLEC4F-specific siRNA, with or without pretreatments with 100 μg/mL Gal or GalNAc polymers. Binding was shown as mean fluorescence intensity (MFI). $n = 3$ experiments. $^*P < 0.05$.

reduced life-span and increased clearance in the liver due to impaired sialylation. Furthermore, our results indicate that Kupffer cells are the major cell-phagocytosing O-glycan–deficient platelets, and hepatocyte AMR facilitates this process.

Increased platelet clearance has been reported in mice lacking sialylation of N-glycans (15, 16). Whether sialylation on O-glycans is important for platelet clearance was unclear, despite the fact that most platelet glycoproteins are modified by core 1-derived O-glycans. Indeed, published data and our analyses reveal that both mouse and human platelets contain high levels of O-glycans, with more sialic acids on platelet O-glycans than on N-glycans (23) (*SI Appendix*, Tables S1 and S2). Previous studies reported that mice with a global deficiency of *C1galt1* or an endothelial/hematopoietic deletion of the *C1galt1* chaperone COSMC (33) display impaired megakaryocyte development and proplatelet formation, leading to reduced peripheral platelet number (33–35). However, it was not clear which O-glycan–deficient cell types contributed to the phenotypes, because these mouse models lack O-glycans not only in blood cells but also in many other tissues including endothelial cells, which are known to be important for megakaryogenesis. In addition, none of these studies examined the role of O-glycans in platelet clearance. We, therefore, bred *C1galt1*$^{f/f}$ with PF4Cre mice, which is a well-established megakaryocyte lineage-specific transgenic Cre mouse line that was successfully used in our laboratory to generate mice with a platelet-specific deletion of *CLEC-2* (3). Unexpectedly, *C1galt1*$^{f/f}$;PF4Cre mice exhibited limited loss of core 1 O-glycans in megakaryocytes and platelets. In a separate study, we found that the C1GALT1 enzyme has a relatively long half-life, which we speculate is the reason why *C1galt1*$^{f/f}$;PF4Cre mice display an incomplete platelet-specific deficiency of O-glycans. To overcome this problem, we generated HC *C1galt1*$^{-/-}$ mice, which lack C1GALT1 specifically in hematopoietic cells, including megakaryocytes and platelets. Thus, this mouse model rules out indirect contributions of O-glycans from other cell types, such as endothelial cells, to platelet homeostasis. HC *C1galt1*$^{-/-}$ mice exhibit reduced peripheral platelet number, impaired platelet sialylation, and increased uptake of platelets by the liver Kupffer cells. These results reveal a function of sialylated O-glycans in platelet clearance in the circulation.

AMR-expressing hepatocytes play an important role in the clearance of desialylated platelets. AMR has been reported to recognize desialylated platelets and mediate phagocytosis of desialylated platelets by hepatocytes (7, 13, 15, 16). Although we observe differential accumulation of HC *C1galt1*$^{-/-}$ platelets in the liver by confocal microscopy, these platelets were rarely found to be associated with or inside hepatocytes. Consistent with these imaging results, our in vitro assay did not detect HepG2 cell ingestion of HC *C1galt1*$^{-/-}$ platelets, even though HC *C1galt1*$^{-/-}$ platelets bind to HepG2 cells. In contrast, we found that HC *C1galt1*$^{-/-}$ platelets were primarily phagocytosed by Kupffer cells, which was partially dependent on AMR. However, we did not detect its mRNA transcripts and protein in purified Kupffer cells, consistent with the finding that AMR is not expressed in human Kupffer cells (36). Thus, these results support that AMR indirectly mediates the phagocytosis of HC *C1galt1*$^{-/-}$ platelets by Kupffer cells.

To determine whether Kupffer cells specifically phagocytose HC *C1galt1*$^{-/-}$ platelets, we compared the clearance of transfused HC *C1galt1*$^{-/-}$ platelets with desialylated platelets, which lack sialic acids on both N- and O-glycans after treatment with α2-3,6,8-neuraminidase, in WT recipient livers. Our conventional confocal-imaging results reveal that both HC *C1galt1*$^{-/-}$ and desialylated platelets are primarily associated with or inside of Kupffer cells. Further spinning-disk confocal intravital microscopy analysis show that either HC *C1galt1*$^{-/-}$ or desialylated platelets interact with and are phagocytosed by Kupffer cells after being transfused. Indeed, previous studies have shown that hepatocytes can only phagocytize particles less than 7.8 nm in diameter (37). The size of liver sinusoidal endothelial fenestrate is about 100 nm (38), which presumably are not big enough for platelets to go through readily. In contrast, about 30% of liver sinusoids consist of Kupffer cells, which can directly interact with platelets. Therefore, our experiments indicate that Kupffer cells

are a major cell type clearing HC *C1galt1*$^{-/-}$ or desialylated platelets.

Kupffer cells express αMβ2 integrin, which plays a role in clearance of chilled platelets by binding to terminal clustered GlcNAc on GPIbα (39). Kupffer cells also express CLEC4F, which binds to glycoproteins carrying terminal Gal or GalNAc (32). However, the role of this interaction in platelet clearance has not been studied. Our data show that Kupffer cell CLEC4F is a major receptor for capturing desialylated or HC *C1galt1*$^{-/-}$ platelets. A previous scanning electron microscopy study revealed that hepatocyte microvilli, which express AMR, are present in the liver sinusoid lumen through sinusoid endothelial fenestrae (40). Thus, our results and published studies support a model in which free-flowing desialylated or HC *C1galt1*$^{-/-}$ platelets adhere to and roll on AMR on hepatocyte microvilli under flow conditions, which facilitates their capture by phagocytic Kupffer cells through the CLEC4F receptor (*SI Appendix*, Fig. S12). This model resembles the P-selectin–mediated initial tether/capture of leukocyte to endothelium in the leukocyte adhesion cascade (41). Future studies are required to address how AMR-expressing hepatocytes cooperate with Kupffer cells for platelet clearance and how CLEC4F receptor mediates phagocytosis of desialylated WT or HC *C1galt1*$^{-/-}$ platelets by Kupffer cells.

A rare autoimmune disease named Tn syndrome is caused by defective core 1 O-glycosylation arising from somatic mutations in C1galt1-specific chaperone Cosmc in a subpopulation of hematopoietic stem cells (42, 43). Patients with Tn syndrome exhibit moderate thrombocytopenia, leukopenia, and anemia. In contrast, severe thrombocytopenia accompanied by the occasional presence of giant platelets is the primary phenotype of HC *C1galt1*$^{-/-}$ mice. Although our study likely provides mechanistic insights into thrombocytopenia in Tn syndrome, further studies are needed to determine the phenotypic discrepancies between Tn syndrome and our mouse model. It also remains to be determined whether or how defective platelet O-glycosylation contributes to the pathogenesis of other disorders with thrombocytopenia such as sepsis and immune thrombocytopenia refractory to splenectomy.

Materials and Methods

Animal studies were approved by Oklahoma Medical Research Foundation's Institutional Animal Care and Use Committee. Mice lacking hematopoietic *C1galt1* were generated as described previously (25). All mice were of C57BL/6J congenic background and kept in a specific-pathogen–free facility. Detailed methods and statistics are given in *SI Appendix, SI Materials and Methods*.

ACKNOWLEDGMENTS. This work was supported by grants from the National Institutes of Health (GM114731, HL128390, HD083418, 1S10OD018530, and P41GM10349010), National Natural Science Foundation of China (81520108005, 81470825, and 81370617), China Scholarship Council, Jiangsu Provincial Special Program of Medical Science (BL2012005), Jiangsu Province's Key Medical Center (ZX201102), The Priority Academic Program Development of Jiangsu Higher Education Institutions, and Jiangsu Province's Key Medical Center (ZX201102).

1. de Gaetano G (2001) Historical overview of the role of platelets in hemostasis and thrombosis. *Haematologica* 86:349–356.
2. Bertozzi CC, et al. (2010) Platelets regulate lymphatic vascular development through CLEC-2-SLP-76 signaling. *Blood* 116:661–670.
3. Herzog BH, et al. (2013) Podoplanin maintains high endothelial venule integrity by interacting with platelet CLEC-2. *Nature* 502:105–109.
4. Morrell CN, Aggrey AA, Chapman LM, Modjeski KL (2014) Emerging roles for platelets as immune and inflammatory cells. *Blood* 123:2759–2767.
5. Harker LA (1977) The kinetics of platelet production and destruction in man. *Clin Haematol* 6:671–693.
6. He R, Reid DM, Jones CE, Shulman NR (1995) Extracellular epitopes of platelet glycoprotein Ib alpha reactive with serum antibodies from patients with chronic idiopathic thrombocytopenic purpura. *Blood* 86:3789–3796.
7. Li J, et al. (2015) Desialylation is a mechanism of Fc-independent platelet clearance and a therapeutic target in immune thrombocytopenia. *Nat Commun* 6:7737.
8. Stasi R, et al. (2008) Analysis of regulatory T-cell changes in patients with idiopathic thrombocytopenic purpura receiving B cell-depleting therapy with rituximab. *Blood* 112:1147–1150.
9. Goette NP, et al. (2016) Platelet apoptosis in adult immune thrombocytopenia: Insights into the mechanism of damage triggered by auto-antibodies. *PLoS One* 11: e0160563.
10. Mason KD, et al. (2007) Programmed anuclear cell death delimits platelet life span. *Cell* 128:1173–1186.
11. Ellies LG, et al. (2002) Sialyltransferase ST3Gal-IV operates as a dominant modifier of hemostasis by concealing asialoglycoprotein receptor ligands. *Proc Natl Acad Sci USA* 99:10042–10047.
12. Grewal PK, et al. (2013) Inducing host protection in pneumococcal sepsis by preactivation of the Ashwell-Morell receptor. *Proc Natl Acad Sci USA* 110:20218–20223.
13. Grewal PK, et al. (2008) The Ashwell receptor mitigates the lethal coagulopathy of sepsis. *Nat Med* 14:648–655.
14. Jansen AJ, et al. (2012) Desialylation accelerates platelet clearance after refrigeration and initiates GPIbα metalloproteinase-mediated cleavage in mice. *Blood* 119:1263–1273.
15. Rumjantseva V, et al. (2009) Dual roles for hepatic lectin receptors in the clearance of chilled platelets. *Nat Med* 15:1273–1280.
16. Sørensen AL, et al. (2009) Role of sialic acid for platelet life span: Exposure of beta-galactose results in the rapid clearance of platelets from the circulation by asialoglycoprotein receptor-expressing liver macrophages and hepatocytes. *Blood* 114:1645–1654.
17. Kauskot A, Hoylaerts MF (2012) Platelet receptors. *Handb Exp Pharmacol* 210:23–57.
18. Lewandrowski U, Moebius J, Walter U, Sickmann A (2006) Elucidation of N-glycosylation sites on human platelet proteins: A glycoproteomic approach. *Mol Cell Proteomics* 5:226–233.
19. Lewandrowski U, et al. (2009) Platelet membrane proteomics: A novel repository for functional research. *Blood* 114:e10–e19.
20. Wilhelm M, et al. (2014) Mass-spectrometry-based draft of the human proteome. *Nature* 509:582–587.
21. Coombs PJ, Taylor ME, Drickamer K (2006) Two categories of mammalian galactose-binding receptors distinguished by glycan array profiling. *Glycobiology* 16:1C–7C.
22. Lopez JA, et al. (1987) Cloning of the α chain of human platelet glycoprotein Ib: A transmembrane protein with homology to leucine-rich α_2-glycoprotein. *Proc Natl Acad Sci USA* 84:5615–5619.
23. King SL, et al. (2017) Characterizing the O-glycosylation landscape of human plasma, platelets, and endothelial cells. *Blood Adv* 1:429–442.
24. Xia L, et al. (2004) Defective angiogenesis and fatal embryonic hemorrhage in mice lacking core 1-derived O-glycans. *J Cell Biol* 164:451–459.
25. Fu J, et al. (2008) Endothelial cell O-glycan deficiency causes blood/lymphatic misconnections and consequent fatty liver disease in mice. *J Clin Invest* 118:3725–3737.
26. Fu J, et al. (2011) Loss of intestinal core 1-derived O-glycans causes spontaneous colitis in mice. *J Clin Invest* 121:1657–1666.
27. Ju T, Cummings RD, Canfield WM (2002) Purification, characterization, and subunit structure of rat core 1 β1,3-galactosyltransferase. *J Biol Chem* 277:169–177.
28. Pan Y, et al. (2014) Podoplanin requires sialylated O-glycans for stable expression on lymphatic endothelial cells and for interaction with platelets. *Blood* 124:3656–3665.
29. Xia L, McEver RP (2006) Targeted disruption of the gene encoding core 1 β1-3-galactosyltransferase (T-synthase) causes embryonic lethality and defective angiogenesis in mice. *Methods Enzymol* 416:314–331.
30. Geisler C, Jarvis DL (2011) Effective glycoanalysis with *Maackia amurensis* lectins requires a clear understanding of their binding specificities. *Glycobiology* 21:988–993.
31. Ravanat C, et al. (2010) A central role of GPIb-IX in the procoagulant function of platelets that is independent of the 45-kDa GPIbalpha N-terminal extracellular domain. *Blood* 116:1157–1164.
32. Yang CY, et al. (2013) CLEC4F is an inducible C-type lectin in F4/80-positive cells and is involved in alpha-galactosylceramide presentation in liver. *PLoS One* 8:e65070.
33. Wang Y, et al. (2012) Platelet biogenesis and functions require correct protein O-glycosylation. *Proc Natl Acad Sci USA* 109:16143–16148.
34. Alexander WS, et al. (2006) Thrombocytopenia and kidney disease in mice with a mutation in the *C1galt1* gene. *Proc Natl Acad Sci USA* 103:16442–16447.
35. Kudo T, et al. (2013) C1galt1-deficient mice exhibit thrombocytopenia due to abnormal terminal differentiation of megakaryocytes. *Blood* 122:1649–1657.
36. Werner M, et al. (2015) All-in-one: Advanced preparation of human parenchymal and non-parenchymal liver cells. *PLoS One* 10:e0138655.
37. Schlepper-Schäfer J, et al. (1986) Endocytosis via galactose receptors in vivo. Ligand size directs uptake by hepatocytes and/or liver macrophages. *Exp Cell Res* 165:494–506.
38. Braet F, Wisse E (2002) Structural and functional aspects of liver sinusoidal endothelial cell fenestrae: A review. *Comp Hepatol* 1:1.
39. Hoffmeister KM, et al. (2003) Glycosylation restores survival of chilled blood platelets. *Science* 301:1531–1534.
40. Warren A, et al. (2006) T lymphocytes interact with hepatocytes through fenestrations in murine liver sinusoidal endothelial cells. *Hepatology* 44:1182–1190.
41. Yago T, et al. (2015) Multi-inhibitory effects of A2A adenosine receptor signaling on neutrophil adhesion under flow. *J Immunol* 195:3880–3889.
42. Cartron JP, Nurden AT (1979) Galactosyltransferase and membrane glycoprotein abnormality in human platelets from Tn-syndrome donors. *Nature* 282:621–623.
43. Nurden AT, et al. (1982) Surface modifications in the platelets of a patient with alpha-*N*-acetyl-D-galactosamine residues, the Tn-syndrome. *J Clin Invest* 70:1281–1291.